Chin. Sci. Bull. (2014) 59(31):4137–4141
DOI 10.1007/s11434-014-0569-y

csb.scichina.com
www.springer.com/scp

Article

Fluid Mechanics

Entropy and its application in turbulence modeling

Rui Zhao · Jili Rong · Xinliang Li

Received: 12 October 2013 / Accepted: 18 March 2014 / Published online: 31 July 2014

Abstract The entropy concept was introduced into the turbulence modeling strategy in the present work. First, the turbulent boundary-layer was described from the point of energy dissipation. Based on the theoretical analysis and direct numerical simulations, the relationship between the entropy increment and viscosity dissipation was systematically investigated. Then, an entropy function f_s was proposed to distinguish the turbulent boundary-layer from the external flow. This function is universal, independent of the inflow conditions or any specific turbulence model. With this function, a new version of delayed-detached-eddy simulation method SDES was constructed and verified with the supersonic boundary-layer flow and the cavity-ramped flow. Initial results showed that this method could successfully avoid the modeled stress depletion problem inherited from the original DES method.

Keywords Entropy · Turbulence boundary-layer · Turbulence modeling · RANS/LES hybrid method

1 Introduction

Entropy, in addition to energy, is an essential physical quantity in thermodynamics. It serves as a measure of the irreversibility of a process and a criterion describing the thermal equilibrium of a system. Because of its general features, the entropy concept has been extended to many other fields, such as thermodynamic optimization and computational techniques [1–6].

As for the turbulent flow, McEligot et al. [7] concluded that about two-thirds or more of entropy generation occurs in the turbulent boundary-layer and they examined the effects of Reynolds number and streamwise pressure gradients on entropy generation. Moore et al. [8] and other researchers [9, 10] developed a series of numerical models for the turbulent entropy production terms. Recently, Zhao et al. [11] systematically investigated the characteristics of entropy increment in turbulent boundary-layer based on direct numerical simulation (DNS) data. With this concept, they revised the length scale of Baldwin–Lomax model, enhancing its robustness for complex flows. They further proposed an entropy-based shielding function to safely preserve the RANS resolved region in the boundary-layer and constructed a new version of delayed-detached-eddy simulation method SDES to avoid the modeled stress depletion (MSD) problem [12]. Although the recent achievements have revealed another potential capability of entropy in turbulence modeling, the definition of entropy expression for turbulent boundary-layer is still not comprehensive. This paper continues to extend the competence of the entropy concept for both compressible and incompressible flows and revisits the SDES method in particular.

Virtually, all flows of practical engineering interests are turbulent. Due to the irregular motion of turbulence, the transportations of mass, momentum, and energy are enhanced, while extra-energy is dissipated. In the near-wall region, as for the fierce turbulent fluctuation and wall frication, a portion of mechanical energy is irreversibly transformed into internal energy, i.e., the entropy increases. Following McEligot et al. [7], we here define turbulence

R. Zhao (✉) · J. Rong
School of Aerospace Engineering, Beijing Institute of Technology, Beijing 100081, China
e-mail: zr@bit.edu.cn

X. Li
Key Laboratory of High Temperature Gas Dynamics, Institute of Mechanics, Chinese Academy of Sciences, Beijing 100190, China

boundary-layer as the region where the local entropy generation rate caused by viscous dissipation is the most significant.

2 Theoretical foundation

With the above definition in mind, the quantitative behavior of entropy increment caused by the viscous dissipation is analyzed. The specific form of entropy s, i.e., entropy per unit mass (J/(K kg)) is both a state and process variable [9]. For compressible flows, the state function of entropy can be obtained from Gibbs equation as follows:

$$\Delta s = c_\mathrm{v}\ln\frac{T}{T_\infty} - R\ln\frac{\rho}{\rho_\infty} = c_\mathrm{v}\ln\left[\frac{p}{p_\infty}\left(\frac{\rho_\infty}{\rho}\right)^\gamma\right], \tag{1}$$

where $c_\mathrm{v} = R/(\gamma - 1)$ is the specific heat at constant volume, R is the gas constant, $\gamma = 1.4$ is the specific heat ratio, and T, p, and ρ are the local temperature, pressure, and density, respectively, subscript ∞ means the quantity in the far field. For incompressible flows, s can be expressed by

$$\Delta s = c_\mathrm{v}\ln\frac{T}{T_\infty}. \tag{2}$$

On the other hand, the balance equation of s is written as follows [9]:

$$\mathrm{d}s = \underbrace{\frac{1}{\rho}\frac{\partial}{\partial x_j}\left(\frac{-q_j}{T}\right)\mathrm{d}t}_{\mathrm{d}s_\mathrm{c}} + \underbrace{\frac{\psi}{\rho T}\mathrm{d}t}_{\mathrm{d}s_T} + \underbrace{\frac{\Phi}{\rho T}\mathrm{d}t}_{\mathrm{d}s_\mu}, \tag{3}$$

where $q_j = k\frac{\partial T}{\partial x_j}$ is the heat transfer, $k = \frac{\mu\gamma R}{(\gamma-1)Pr}$ is the thermal conductivity, $Pr = 0.7$ is the laminar Prandtl number, $\psi = \frac{k}{T}\left(\frac{\partial T}{\partial x_j}\frac{\partial T}{\partial x_j}\right)$, $\Phi = \frac{\mu}{2}\left(\frac{\partial u_i}{\partial x_j} + \frac{\partial u_j}{\partial x_i}\right)^2$, and μ is the molecular viscosity.

On the right side of Eq. (3), the first term $\mathrm{d}s_\mathrm{c}$ is the thermal conductive term, whose value may be either negative or positive. The other two terms stand for the entropy production terms. $\mathrm{d}s_\mathrm{T}$ represents the entropy generation due to heat transfer across finite temperature gradients, while $\mathrm{d}s_\mu$ represents the local entropy generation by the viscous dissipation. These two positive terms apply to both compressible and incompressible Newtonian fluids [9]. As the term $\mathrm{d}s_\mathrm{c}$ includes the second derivative of T which may cause numerical singularity at the adiabatic wall, we simply neglect this term at this step. By combing Eq. (3) with (1) or (2) (depending on the flow condition), the entropy increment caused by the viscous dissipation can be deduced as follows:

$$\Delta s_\mathrm{vis} = \frac{\mathrm{d}s_\mu}{\mathrm{d}s_\mathrm{T} + \mathrm{d}s_\mu}\times\Delta s = \frac{\Phi}{\Phi + \psi}\times\Delta s. \tag{4}$$

For turbulent flows, Eq. (4) is Reynolds-averaged and the turbulent terms are modeled with the Moore model [8]:

$$\Delta\bar{s}_\mathrm{vis} = \frac{(1+\mu_\mathrm{t}/\mu)\bar{\Phi}}{(1+\mu_\mathrm{t}/\mu)\bar{\Phi} + (1+k_\mathrm{t}/k)\bar{\psi}}\times\Delta\bar{s} = \frac{\bar{\Phi}}{\bar{\Phi} + \alpha\bar{\psi}}\times\Delta\bar{s}, \tag{5}$$

in which $\alpha = \frac{\mu Pr_\mathrm{t} + \mu_\mathrm{t}Pr}{\mu Pr_\mathrm{t} + \mu_\mathrm{t}Pr_\mathrm{t}}$, $Pr_\mathrm{t} = 0.9$ is turbulent Prandtl number, μ_t is the turbulent viscosity, and the instantaneous variables in $\bar{\Phi}$, $\bar{\psi}$, $\Delta\bar{s}$ are replaced with the corresponding averaged one, respectively.

When the potential flows pass the wall, the mechanical energy is dissipated to zero due to the viscous frication. Naturally, the value of $\Delta\bar{s}_\mathrm{vis}$ at the wall is directly related to inflow speeds, i.e., it varies orders of magnitude from the low-speed flows to hypersonic flows. In order to obtain $\Delta\bar{s}_\mathrm{vis}$ normalized for modeling convenience, the following procedures are taken.

For adiabatic boundary-layer flows, the maximum entropy increment could be expressed as follows [13]:

$$\Delta s_\mathrm{max} = c_\mathrm{v}\ln\left[\frac{p_\infty}{p_\mathrm{w}}\times\left(1 + \frac{\gamma-1}{2}Ma_\infty^2\right)^\gamma\right], \tag{6}$$

where the subscript w means the quantity at the wall. Since $p_\infty < p_\mathrm{w}$ in general, we simplify Eq. (6) and assume Δs_max as follows:

$$\Delta s_\mathrm{max} = c_\mathrm{v}\ln\left(1 + \frac{\gamma-1}{2}Ma_\infty^2\right)^\gamma. \tag{7}$$

With $\Delta\bar{s}_\mathrm{vis}$ normalized by Δs_max (Eq. (7)), a novel entropy concept, named entropy increment ratio $\bar{s}_\mathrm{vis}$, is proposed:

$$\bar{s}_\mathrm{vis} = \frac{\Delta\bar{s}_\mathrm{vis}}{\Delta s_\mathrm{max}} = \frac{\bar{\Phi}}{\bar{\Phi} + \alpha\bar{\psi}}\times\frac{\Delta\bar{s}}{\Delta s_\mathrm{max}}. \tag{8}$$

$\bar{s}_\mathrm{vis}$ represents the viscous dissipation rate of per unit mechanic energy, whose behavior is systematically investigated based on the DNS data (Table 1). Figure 1 compares the profiles of $\bar{s}_\mathrm{vis}$ and the streamwise velocity $\bar{u}$ normal to the wall with different inflow Mach numbers. The profile of $\bar{s}_\mathrm{vis}$ depicts a consistent trend as that of the velocity $\bar{u}$, and the boundary-layer region is well represented by $\bar{s}_\mathrm{vis} > 0$. Moreover, the value of $\bar{s}_\mathrm{vis}$

Table 1 Simulation conditions for the boundary-layer flows (DNS)

	Ma	Re	T_w/T_∞	$T_\mathrm{w}/T_\mathrm{r}$
Case 1	0.7	5.0×10^4	1.098	1.003
Case 2	2.25	6.35×10^5	1.9	0.961
Case 3	6	2.0×10^6	6.98	0.878

Ma inflow Mach number, Re Reynolds number per inch, T_w wall temperature, T_∞ inflow temperature, and T_r recovery temperature

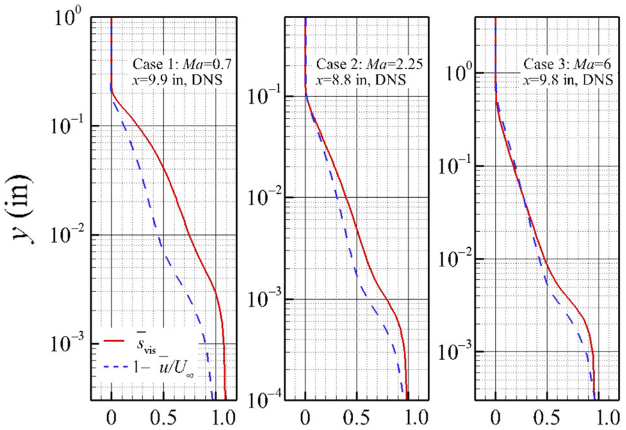

Fig. 1 Entropy increment ratio and velocity profiles normal to the wall of different Mach numbers (DNS results)

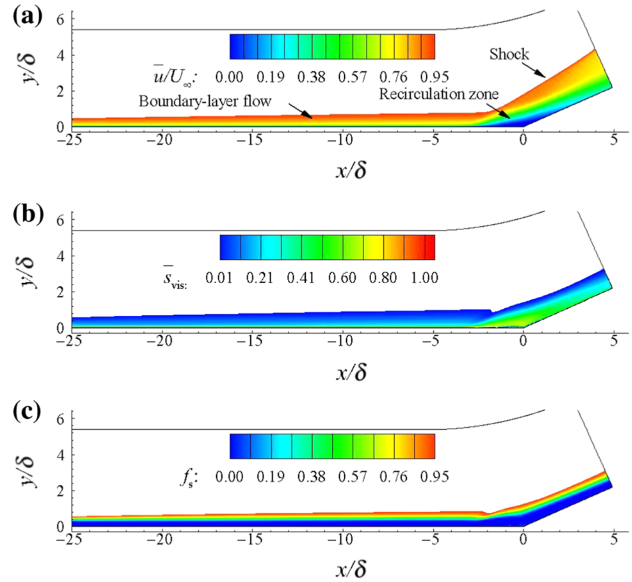

Fig. 2 Distributions of streamwise velocity $\bar{u}$ (only depict $\bar{u}/U_\infty$<0.95) (**a**), entropy increment ratio $\bar{s}_{\rm vis}$ (only depict $\bar{s}_{\rm vis}>0.01$) (**b**) and entropy function $f_{\rm s}$ (only depict $f_{\rm s}$<0.95) (**c**) along the compression ramp

approaches unity toward the wall. This character is convenient as the weak dependence of models or physical parameters on flow conditions is always desired.

Remember that entropy may also increase in other regions, such as the areas where shock waves and detached vortex exist. To avoid this defect, an entropy function is proposed to confine the predicted turbulent boundary-layer near the wall:

$$f_{\rm s}=1.0-\tanh\left(\bar{s}_{\rm vis}/l_{\rm s}^{3}\right), \tag{9}$$

where $l_{\rm s}$ is the length-scale ratio, which is designed to be less than 1.0 in the boundary-layer and increase quickly in the external flows. We construct $l_{\rm s}$ following the spirit of DES97 [14], but with minor revision:

$$l_{\rm s}=\begin{cases} C_{\rm s}f(a_1,a_2)d/C_{\rm DES}\Delta, & \bar{s}_{\rm vis}>0.05,\\ d/C_{\rm DES}\Delta, & \text{otherwise,}\end{cases} \tag{10}$$

in which $C_{\rm s}$ = 0.12 is an empirical constant, $f(a_1,a_2)$ is an anisotropic function recommended by Scotti et al. [15], d is the distance normal to the wall, $C_{\rm DES}$ = 0.65, and Δ is the grid spacing defined by $\Delta=\max(\Delta x,\Delta y,\Delta z)$.

The distributions of $\bar{u}$, $\bar{s}_{\rm vis}$ and $f_{\rm s}$ are investigated in the 24° supersonic compression corner flow (DNS) [11]. As Fig. 2 indicates, the general velocity criterion ($\bar{u}/U_\infty$ < 95 % or 99 %) fails to denote the boundary-layer range, especially in the corner area where the velocity is decelerated by shocks. Comparatively, the turbulent boundary-layer predicted by $\bar{s}_{\rm vis}$ and $f_{\rm s}$ based on the viscosity dissipation is more reasonable.

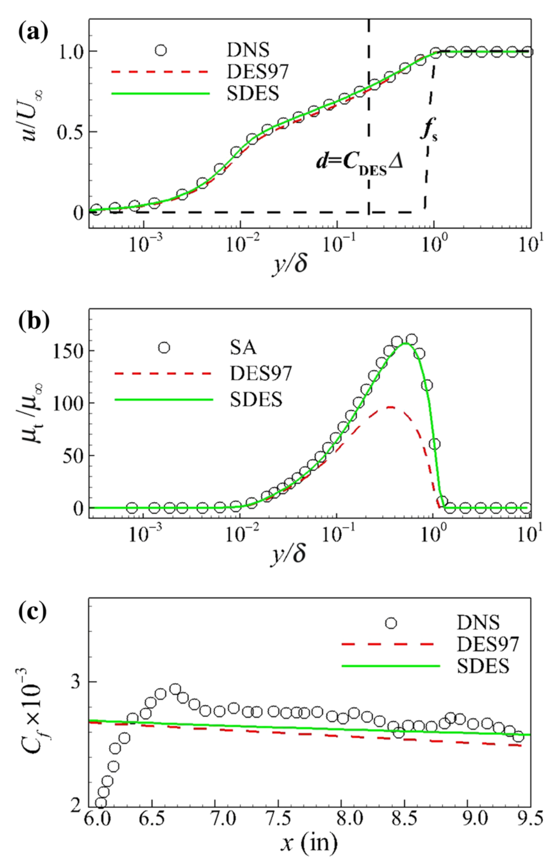

Fig. 3 DES97 and SDES in the boundary-layer flow. **a** Time-averaged velocity and $f_{\rm s}$ profiles along the wall-normal direction (x=8.8 in), **b** time-averaged eddy viscosity profiles along the wall-normal direction (x=8.8 in), and **c** time-averaged wall-friction coefficient along the streamwise direction (x-direction)

3 Entropy-based DES method

Since entropy function $f_{\rm s}$ could denote the turbulent boundary-layer physically, it is applied as a shielding function with the length scale $\tilde{d}$ in DES97 redefined as follows:

$$\tilde{d} = d - f_s \max(0, d - C_{DES}\Delta). \quad (11)$$

The performance of this entropy-based DES method (named SDES) is investigated preliminarily. Figure 3 compares the results of DES97 and SDES with SA-RANS [16] and DNS in the supersonic boundary-layer flow (Case 2 in Table 1). The grid resolution ranges between the classical values used in LES and RANS simulations, in order to exhibit the MSD problem. With this ambiguous grid, the RANS reserved range ($d < C_{DES}\Delta$) in DES97 only holds 20 % of the boundary-layer (Fig. 3a). Since the near-wall grid is not fine enough to directly resolve the turbulent fluctuation, the modeled Reynolds stresses predicted by DES97 are lacked. As Fig. 3 shows, DES97 underestimate the eddy viscosity by almost 40 % (Fig. 3b), while the velocity profiles slightly depart from that of DNS at the log-law region (Fig. 3a). With the thickness of the boundary-layer increasing along the streamwise direction, the wall-frication coefficient predicted by DES97 becomes much lower than DNS (Fig. 3c). On the other side, the shielding function f_s in SDES accurately denotes the whole layer (Fig. 3a) and the MSD problem is greatly alleviated. Thus, the results of SDES agree well with DNS data.

Figure 4 shows details of DES97 and SDES resolutions in the cavity-ramp flow [12]. The grid around the cavity area is refined to capture the free-shear layer structure (Fig. 4a, b), so is the grid in the ramped portion for the

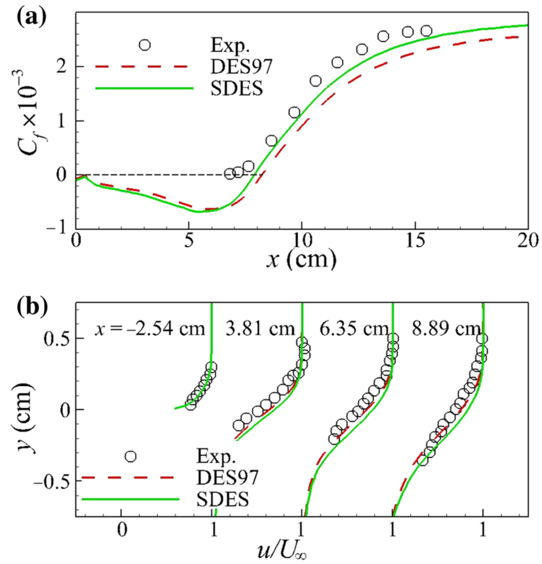

Fig. 5 Time-averaged skin-frication coefficients (**a**) and streamwise velocity (**b**) distributions

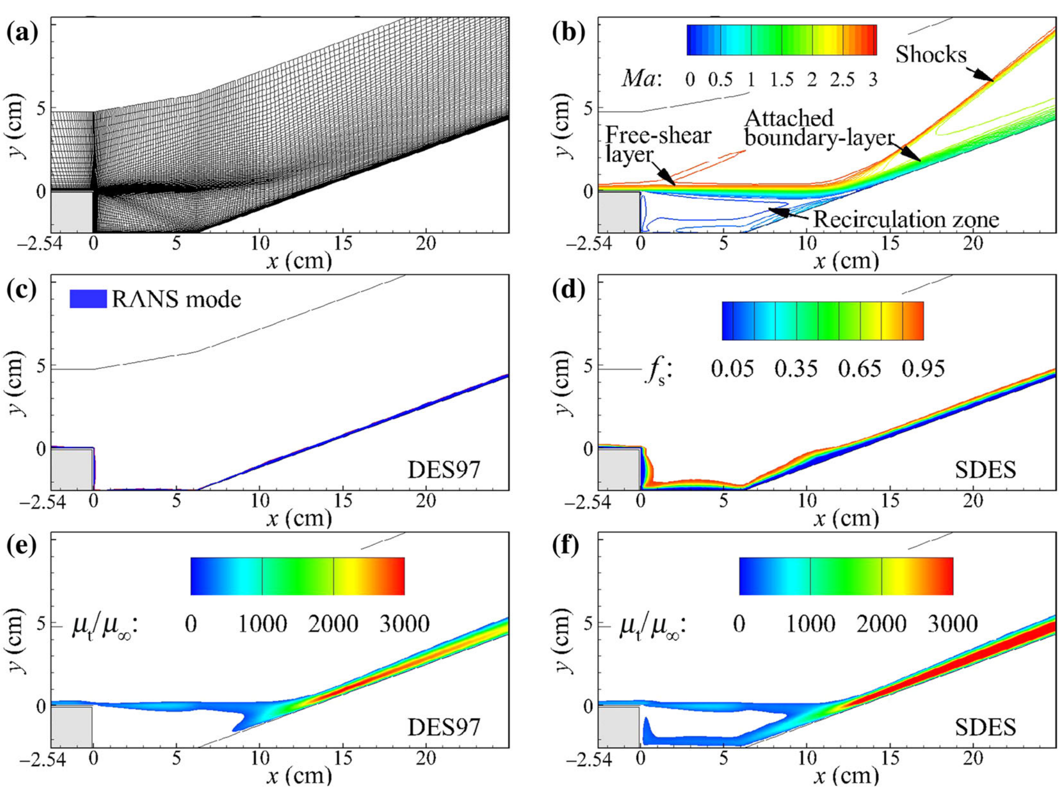

Fig. 4 DES97 and SDES over the cavity ramp. **a** Grid, **b** time-averaged flowfield, **c** RANS reserved region in DES97, **d** time-averaged entropy function f_s in SDES (only depict $f_s < 0.95$), and **e**, **f** time-averaged turbulent viscosity obtained by DES97 and SDES, respectively (only depict $\mu_t/\mu_\infty > 200$)

recovering boundary-layer. Therefore, the RANS modeled area where $d < C_{DES}\Delta$ in DES97 becomes inadequate in the above regions (Fig. 4c). In contrast, the proposed entropy function f_s in SDES could reliably indicate the boundary-layer development (Fig. 4d), resulting in a more prominent level of eddy viscosity distribution (Fig. 4e, f). The error of the predicted length of the recirculation zone is 8.6 % larger than the experimental data for DES97, which is reduced by 50 % for SDES (Fig. 5a). Since the rise of wall frication indicates the rate of recovery of the boundary-layer downstream of reattachment, the recovering streamwise velocity of SDES develops more quickly than DES97 (Fig. 5b).

4 Conclusion

In summary, a normalized entropy concept—entropy increment ratio $\bar{s}_{vis}$—was deduced in this paper. It serves as a pivotal parameter in the function f_s to reliably denote the turbulent boundary-layer from the point of energy dissipation. Through employing f_s as a shielding function, a novel hybrid strategy (SDES) was revisited and showed the superiority over DES97 in the simulation of supersonic cavity-ramp flow. Although it is not necessarily the best formulation available, the present one for f_s appears simple and general enough to be recommended in the turbulence modeling related to the boundary-layer. Nevertheless, the effect of the neglected term ds_c which is important in hypersonic flows with remarkable wall-heat convection is left for further investigations.

Acknowledgment This work was supported by the National Basic Research Program of China (2009CB724104) and Civil Aerospace Technology Advanced Research Project. The authors are grateful for Dr. Wu Peng in Belgium for critical reading of this manuscript.

References

1. Hu GJ, Cao BY, Guo ZY (2011) Entransy and entropy revisited. Chin Sci Bull 27:2974–2977
2. Chen X, Xuan YM, Han YG (2010) Investigation of the entropy generation and efficiency of as solar thermophotovoltaic system. Chin Sci Bull 55:3718–3726
3. Naterer GF, Camberos JA (2001) The role of entropy and the second law in computational thermofluids. AIAA-2001-2758
4. Naterer GF, Camberos JA (2003) Entropy and the second law fluid flow and heat transfer simulation. J Thermophys Heat Transf 17:360–371
5. Gillian HB, Mark JL (2011) Principle of minimum entropy analysis applied to unsteady flow in hypersonic three-dimensional inlets. AIAA-2011-2307
6. Guermond JL, Pasquetti R, Popov B (2011) Entropy viscosity for nonlinear conservation equations. J Comput Phys 230:4248–4267
7. McEligot DM, Walsh EJ, Laurien E et al (2008) Entropy generation in the viscous parts of turbulent boundary layers. J Fluids Engrg 130:61205
8. Moore J, Moore JG (1983) Entropy production rates from viscous flow calculations, Part I. a turbulent boundary layer flow. ASME Paper 83-GT-70, ASME Gas Turbine Conference, Phoenix, AZ
9. Adeyinka OB, Naterer GF (2004) Modeling of entropy production in turbulent flows. J Fluids Engrg 126:893–899
10. Kock F, Herwig H (2005) Entropy production calculation for turbulent shear flows and their implementation in CFD codes. Int J Heat Fluid Flow 26:672–680
11. Zhao R, Yan C, Yu J et al (2013) Improvement of Baldwin-Lomax turbulence model for supersonic complex flow. Chin J Aeronaut 26:529–534
12. Zhao R, Yan C, Li XL et al (2013) Towards an entropy-based detached eddy simulation. Sci China Phys Mech Astron 56:1970–1980
13. Walz A (1969) Boundary layers of flow and temperature. MIT Press, Cambridge
14. Spalart PR, Jou WH, Allmaras SR (1998) Comments on the feasibility of LES for wings, and on a hybrid RANS/LES approach. Proceedings of the 1st AFSOR international Conference on DNS/LES, Greyden Press, Columbus, OH, pp 137−147
15. Scotti A, Meneveau C, Lilly DK (1993) Generalized smagorinsky model for anisotropic grids. Phys Fluids A 5:2306–2308
16. Spalart PR, Allmaras SR (1992) A one-equation turbulence model for aerodynamic flows. AIAA-92-0439